

A comparative study of toluene catalytic oxidation over cerium/TiO₂ (anatase) and vanadium/TiO₂ (anatase) catalysts

Attera Worayingyong,* Anwaraporn Niltharach and Yingyot Poo-arporn

Department of Chemistry, Faculty of Science, Kasetsart University, Bangkok 10903, Thailand.

* Corresponding author, E-mail: fsciarw@ku.ac.th

Received 28 Apr 2004
Accepted 27 Sep 2004

ABSTRACT: Cerium and vanadium species supported on TiO₂ (anatase) were prepared by sol-gel formation, with the same contents of cerium (or vanadium) to titanium (in TiO₂), and calcined at 723 or 823 K. The X-ray diffraction (XRD) patterns of the supported vanadium species showed mainly the anatase phase of TiO₂, whereas the cerium species formed a less crystalline anatase phase. The X-ray photoemission spectroscopic (XPS) results proved V(V) and V(IV) in all vanadium samples; all cerium samples had a significant proportion of Ce(III). The catalytic activities of the cerium species were comparable to those of the well known vanadium species when the same mole ratio of the prepared catalysts was used in the catalytic oxidation of toluene. It is assumed that oxygen in the M-O-Ti bonds (M = Ce or V) together with the high oxidation states of Ce(IV) and V(V) play an important role in the oxygen transfer step of the oxidation reactions. The product selectivities from the high performance catalysts showed that the cerium/TiO₂(anatase) was active for aromatic destruction, whereas the partially deactivated vanadium/TiO₂(anatase) was suitable for partial oxidation of toluene, producing benzaldehyde as a major product.

KEYWORDS: V/TiO₂ (anatase), Ce/TiO₂ (anatase), titanium oxide, oxidative catalyst.

INTRODUCTION

The dispersion of vanadium species on TiO₂ (anatase) has been studied extensively. Supported vanadium oxide catalysts have been used in the oxidative dehydrogenation of organic compounds, the selective catalytic reduction (SCR) of nitrogen oxides, and the oxidation of volatile organic compounds (VOCs).¹ Vanadium species supported on TiO₂ perform well in controlling catalytic reactions.² Spectroscopic investigations show that isolated monomeric vanadium species, polymeric 2-D vanadium species and crystalline V₂O₅ coexist on the support, with their relative abundance being related to the vanadium content.¹ The preferred phase of TiO₂ in catalysis is mainly anatase since it is chemically active and suitable for acting as a catalyst and a support.³ A major disadvantage associated with the TiO₂ support is the relatively low thermal stability of the active anatase structure at high temperature.¹ Several attempts have been made to increase catalyst lifetime. Other elements can be added to TiO₂ to improve structural stability. For example, CeO₂ stabilizes the active anatase phase in the dispersed state and improves the resistance to thermal loss of the supported catalyst surface area and the catalytic activity.³ Mixing CeO₂ and TiO₂ at high temperatures

under various conditions can lead to a wealth of mixed compounds, such as Ce₂TiO₅, Ce₂Ti₂O₇, Ce₄Ti₉O₂₄.⁴ In recent years, the CeO₂ content in automotive exhaust catalysts has greatly increased, due to restoring in excess of oxygen.⁵

Toluene is an important feedstock due to its application in industrial processes, such as benzaldehyde and phthalic anhydride production.⁶ It is also a representative of aromatic hydrocarbons categorized as hazardous materials.⁷ Thus, development of methods for the oxidation of aromatics such as toluene, is important for environmental reasons.

Research on this system has concentrated on the study of cerium and vanadium species on the activity of titanium oxide (anatase) for the oxidation of toluene as a representative aromatic. The work was carried out with the goal of studying the influence of the cerium species in comparison to the well known vanadium species supported on titanium oxide (anatase) oxidative catalysts, with the same mole ratio and percentage weight of active component and using the same sol-gel preparative method. The calcination temperatures of the prepared catalysts, 723 and 823 K were chosen according to the temperatures for toluene oxidation. The selectivities for the major toluene oxidation products were also reported.

Table 1. Sample codes for the catalysts studied, with the number of mole ratios and percentage weight for each component.

Sample code	Ti		V		V/Ti	Ce		Ce/Ti
	mol%	w/w	mmol	%w/w	mol/mol	mmol	%w/w	mol/mol
sTiO ₂	0.01	100.00	-	-	-	-	-	-
VTi03	0.01	96.88	0.30	3.12	0.03	-	-	-
VTi22	0.01	77.49	2.70	22.51	0.27	-	-	-
VTi30	0.01	69.66	4.10	30.34	0.41	-	-	-
VTi40	0.01	59.53	6.40	40.47	0.64	-	-	-
CTi03	0.01	96.88	-	-	-	0.10	3.12	0.01
CTi08	0.01	91.94	-	-	-	0.30	8.06	0.03
CTi22	0.01	77.36	-	-	-	1.00	22.64	0.10
CTi30	0.01	68.69	-	-	-	1.60	31.31	0.16
CTi40	0.01	60.16	-	-	-	2.30	39.84	0.23

MATERIALS AND METHODS

Catalyst Preparation

The sol-gel method was employed. Titanium(IV) bis(ethyl acetoacetato)diisopropoxide (Aldrich, tech) and vanadyl acetylacetonate (Fluka, 97%) or cerium nitrate hexahydrate (Fluka, 99.0%) were used according to the mole ratios shown in Table 1. The precursors were stirred in acetylacetone (Fluka, purum) (7 mmol), ethylene glycol (Fluka, purum) (79 mmol), and water (40 mmol) at room temperature. The mixture was allowed to rest in an oven at 348 K for 12-24 h to form gel, which was then dried at 383 K for 24 h to solidification and then calcined in flowing air (100 cm³ min⁻¹) at 723 K for 4 h. Reference chemicals were vanadium(V) oxide (Riedel-deHaën, 99.0%) and cerium(IV) oxide (Aldrich, 99.9%). Reference titanium oxide (anatase) (sTiO₂) was prepared by the sol-gel method described above, without the addition of the cerium or vanadium compound.

Catalyst Characterization

X-ray Diffraction (XRD)

X-ray diffraction experiments were performed on a Philips X'Pert-MPD diffractometer using Cu K α radiation ($\lambda = 1.540 \text{ \AA}$) with an anode current of 30 mA and accelerating voltage of 40 kV, equipped with a curved graphite monochromator. In all diffraction patterns a step size of 0.02 degrees was used. The identification of crystalline phases was accomplished by comparison with JCPDS (Joint Committee on Powder Diffraction Standards) file numbers 75-1537, 41-1426, and 81-0792 for anatase, vanadium oxide and cerium oxide, respectively.

X-ray Photoemission Spectroscopy (XPS)

XPS experiments were carried out at the Siam Photon Laboratory,⁸ using a VG Scientific CLAM 2 energy analyzer. Powder samples were pressed on carbon tape mounted on a molybdenum plate. The

samples were cleaned by 3 kV Ar ion sputtering for 1 hour before analysis. The excitation scan was 300 watt Mg K α and the pass energy of the analyzer was 20 eV. All binding energies were referred to the C1s line at 284.8 eV.

Raman Spectroscopy

The spectra were performed on a MK1 Renishaw Raman Imaging Microscope 160, equipped with a CCD detection system using an argon ion laser (514.5 nm) excited with an incident power of 50 mW.

BET Surface Area Determination

The adsorption isotherms and BET plots were carried out by a Quantachrome Autosorb to determine the catalyst surface areas.

Catalytic Testing

The catalytic activity was tested in a fixed bed, stainless steel micro reactor. A thermocouple was set in the middle of the catalyst bed, that was diluted with chromosorb. Toluene (Mallinckrodt, 99.9 %) was introduced into a vapourizer (383 K) by a peristaltic pump (Masterflex). Products in the reactor outlet were analyzed on-line by a gas chromatograph (Varian CP 3800) with a flame ionization detector, using a column (0.53 mm id x 30 m) packed with CP-wax 52CB on

Table 2. Reaction conditions for the catalytic oxidation of toluene in the presence of the prepared catalysts.

Reaction conditions	Value setting
Temperature, K	723.0
Pressure, kPa	180.0
Mole of toluene, mmol s ⁻¹	0.03
Mole of oxygen, mmol s ⁻¹	0.02
Volume of catalyst, cm ³	0.50
Contact time, s	0.48
GHSV, h ⁻¹	7512

WCOT fused silica. The reaction conditions are given in Table 2.

Before the reaction was started, the catalysts were pretreated in flowing air ($85 \text{ cm}^3 \text{ min}^{-1}$) at 723 K for 1 h (or at 823 K for 3 h). The concentration of toluene was determined by switching to bypass the reactor and subsequently analyzing on line by gas chromatographic method. When a constant concentration was reached, the reaction mixture containing toluene, vapourized at 383 K, mixed with N_2 ($15 \text{ cm}^3 \text{ min}^{-1}$) as carrier gas and flowing air ($85 \text{ cm}^3 \text{ min}^{-1}$), was passed through the catalyst bed in the reactor at 723 K. The product stream was analyzed on line by gas chromatographic method. The analysis results were reported as a function of time (reaction time), during which toluene was oxidized in air in the presence of each tested catalyst. The percentage conversion of toluene was calculated according to the remaining toluene concentration relative to the starting concentration. At the same time, the concentrations of major toluene oxidation products, namely methanol benzene and benzaldehyde were analyzed and calculated relative to the converted toluene concentration. The results were reported as percentage selectivities of methanol benzene and benzaldehyde as a function of reaction time. When the reaction was complete, O_2 (in air) was allowed to pass through the reactor, the temperature of which was initially set at 673 K and increased to 823 K with a 50 K increment per 30 minutes to regenerate the used catalyst. The regenerated catalyst was tested in the second run.

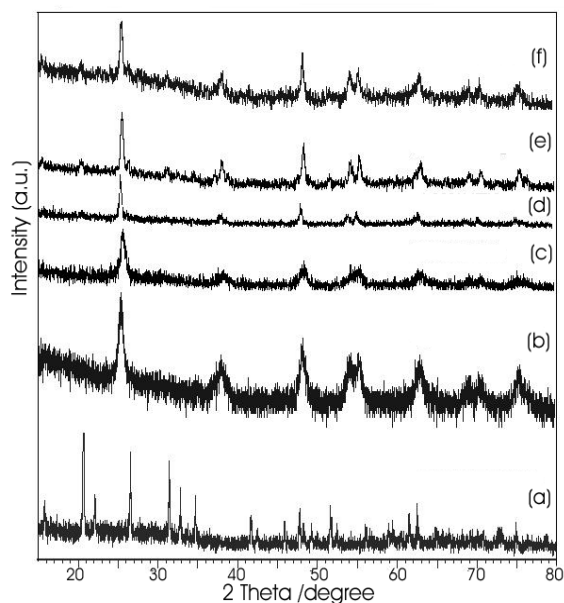


Fig 1. X-ray diffraction patterns of (a) sV₂O₅, (b) sTiO₂, (c) VTi03, (d) VTi22, (e) VTi30 and (f) VTi40, all samples calcined at 723 K.

RESULTS AND DISCUSSION

X-ray Diffraction (XRD) and Raman Spectroscopy

The XRD patterns of the prepared samples of vanadium species on TiO₂ supports (VTi03, VTi22, VTi30 and VTi40) together with reference anatase TiO₂ (sTiO₂) and reference V₂O₅ (sV2O5) are shown in Figure 1. All samples calcined at 723 K showed the presence of the anatase structure of titanium oxide (according to JCPDS PDF No 75-1537) which has distorted TiO₆ octahedra in a tetragonal unit cell.⁹ The samples of higher vanadium loading (VTi30 and VTi40) showed traces of vanadium oxide at 2θ 21.5° and 31.5° (JCPDS PDF No 41-1426). In this experiment, the vanadium oxide peak could not be observed in the XRD pattern even with a vanadium concentration of 22% (VTi22), which agreed well with the literature that there is no significant indication of vanadium oxide if the concentration of the V₂O₅ is less than 15%.¹ The XRD results indicated that the higher loadings (VTi30 and VTi40) had little vanadia dispersed on the TiO₂ (anatase). It has been reported that the dispersed vanadia on the titania support enhanced the crystallization of TiO₂.^{10,11} A phase transformation of anatase to rutile is normally expected at 1073 K for TiO₂ with trace of V₂O₅.¹⁰ In the present study, the calcination temperature was 723 K, with no indication of the rutile phase (JCPDS PDF No 76-1941).

The Raman spectra of the vanadium species on TiO₂ supports (VTi03, VTi22, VTi30 and VTi40) together with reference anatase TiO₂ (sTiO₂) and reference V₂O₅ (sV2O5) are shown in Figure 2. The peaks of TiO₂

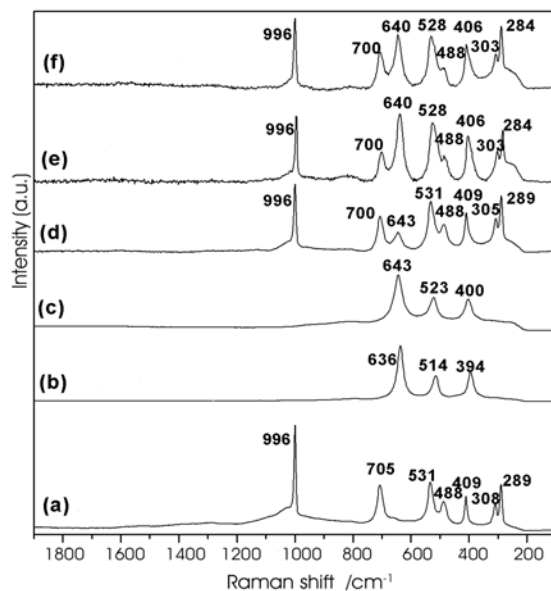


Fig 2. Raman spectra of (a) sV₂O₅, (b) sTiO₂, (c) VTi03, (d) VTi22, (e) VTi30 and (f) VTi40, all samples calcined at 723 K.

at 394, 514 and 636 cm^{-1} are characteristic of the anatase phase of TiO_2 and the peaks at 289, 308, 409, 488, 531, 705 and 996 cm^{-1} are characteristic of the crystalline V_2O_5 .¹² The most intense peak, at 996 cm^{-1} , is due primarily to the symmetric V=O stretch in the bulk.¹² The Raman peaks below 400 cm^{-1} correspond to the bending modes of V-O-V groups. The symmetric and asymmetric stretching modes of the bridging V-O-V groups are observed in the range of 450 to 850 cm^{-1} .¹³

Sample VTi03 showed only the characteristic peaks of anatase, at 394, 514, 636 cm^{-1} , shifted to higher wavenumbers at 400, 523, 643 cm^{-1} , respectively, with some broad bands below 400 cm^{-1} . It is assumed that the Ti-O bonds corresponding to the vertical bonds in the anatase⁹ were shorter in the VTi03 sample, due to interstitial vanadium ions in the hole between the octahedral TiO_6 units forming small amounts of Ti-O-V and V-O-V species. From the results for VTi03 and VTi22, there was no evidence of isolated VO_4^{3-} units for which the Raman shifts lie in the range 830-855 cm^{-1} .¹ Raman spectroscopy suggests that VTi22, VTi30 and VTi40 have a polyvanadate chain. Thus, the V=O groups bonded to the anatase are shown by the intense Raman band at 996 cm^{-1} , while the V-O-V groups are shown by Raman peaks below 400 cm^{-1} resulting from the bending modes, consistent with the results described by Reddy *et al.*¹² The appearance of the Raman peaks of VTi22, VTi30 and VTi40 as the combination of anatase and V_2O_5 peaks confirmed small amounts of crystalline

V_2O_5 on the surface of the anatase phase in the hole between the octahedral TiO_6 units.⁹ However the crystalline V_2O_5 present in all samples could not be detected in the XRD patterns, possibly due to the small amount on the anatase. The morphologies of the vanadium species on the titanium oxide (anatase) can be proposed as follows: (i) the lower loading vanadium species (VTi03) was mainly supported as amorphous with some Ti-O-V and V-O-V bonds; (ii) the vanadium species of the higher loading (VTi22, VTi30 and VTi40) can be assigned to two dimensional polyvanadate species with some small amounts of crystalline V_2O_5 .^{13,14}

The XRD results of cerium species on TiO_2 supports (CTi03, calcined at 723 K; CTi08, CTi22, CTi30 and CTi40, calcined at 823 K), together with reference anatase TiO_2 (sTiO2, calcined at 723 K) and reference CeO_2 (sCeO2) are shown in Figure 3. All samples showed low crystalline anatase due to the cerium species. In particular, the highest cerium loading (CTi40) showed only amorphous TiO_2 (Figure 3, g).

The Raman spectra of the cerium species on TiO_2 supports (CTi03, CTi08, CTi22, CTi30 and CTi40), reference anatase TiO_2 (sTiO2) and reference CeO_2

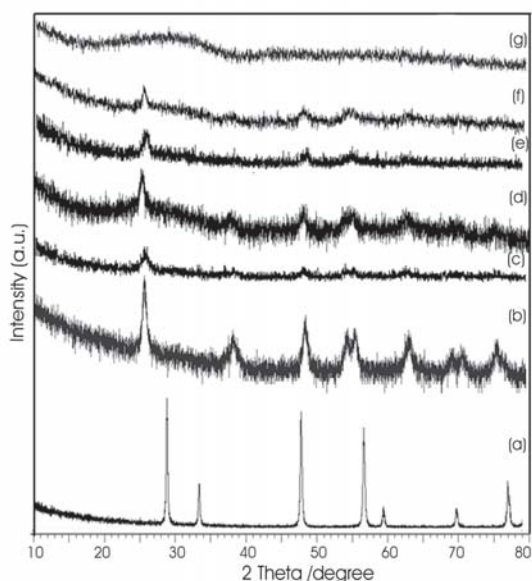


Fig 3. X-ray diffraction patterns of (a) sCeO₂, (b) sTiO₂, (c) CTi03, (d) CTi08, (e) CTi22, (f) CTi30 and (g) CTi40. Samples (b-c) calcined at 723 K and samples (d-g) calcined at 823 K.

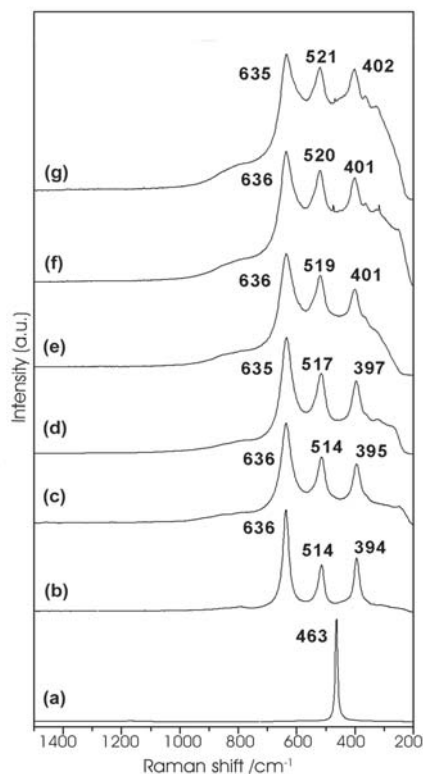


Fig 4. Raman spectra of (a) sCeO₂, (b) sTiO₂, (c) CTi03, (d) CTi08, (e) CTi22, (f) CTi30 and (g) CTi40. Samples (b-c) calcined at 723 K and samples (d-g) calcined at 823 K.

(sCeO₂) are shown in Figure 4. They revealed only the presence of crystalline TiO₂ (anatase). The typically strong Raman shift of cerium oxide at 463 cm⁻¹, due to the characteristic Raman active mode of the fluorite structure,¹¹ was barely recognizable in all cerium samples. The Raman shifts of the TiO₂ (anatase) at 394 and 514 cm⁻¹ appeared at higher wavenumbers at 402 and 521 cm⁻¹, respectively, when TiO₂ (anatase) had the higher cerium content. All samples (CTi03, CTi08, CTi22, CTi30 and CTi40) showed the Raman shifts between 635-636 cm⁻¹, except that the bands were broader and had more shoulder for higher loading samples.

From these results, the lower cerium loading is assumed to place the cerium ions in the cavities between the octahedral TiO₆ unit of anatase. This results in the formation of Ti-O-Ce bonds, which shorten and strengthen the Ti-O bonds of the distorted octahedral units and shifted Raman peaks to higher wavenumbers. The higher loading samples, CTi30 and CTi40, are assumed to have more cerium ions in the hole between the octahedral TiO₆ units, which then form Ce-O-Ce bonds in addition to Ti-O-Ce bonds. The XRD results of TiO₂ mixed with rare earth oxides (0.5%) revealed that these oxides could inhibit the phase transformation during thermal treatment, even with mixtures calcined at moderately high temperatures (<973 K for TiO₂/CeO₂).¹¹ The inhibition of the transition was ascribed to the stabilization of the anatase phase by the surrounding rare earth oxides through the formation of Ti-O-rare earth element bonds,¹¹ which is corresponding to the assumption from the experiment.

X-ray Photoemission Spectroscopy (XPS)

The binding energies (E_b) of V2p_{3/2} were 516.4, 517.9, 516.5 and 516.5 eV, in the samples: the reference V₂O₅ (sV2O5), VTi03, VTi30 and VTi40, respectively (Figure 5), and were relative to that of the value in the literature of V₂O₅ (517.7eV).¹⁵ The observed peaks were broad, especially those of VTi03. The binding energies of V2p_{1/2} were 523.6, 522.9, 522.7 and 523.1 eV, in the samples: the reference V₂O₅ (sV2O5), VTi03, VTi30 and VTi40, respectively (Figure 5). The mean value of energy level differences between the V2p_{3/2} levels and the V2p_{1/2} levels was 6.3 eV. The deconvolutions of the V2p_{3/2} peak of VTi30 and VTi40 showed two peaks at binding energy of 514.2 and 516.5 eV for VTi30, and at binding energy of 514.0 and 516.5 eV for VTi40. A similar result for the V2p peaks for a V₂O₅/La₂O₃-TiO₂ sample has been observed.¹ The V2p_{3/2} binding energy of V₂O₅ [V(V) state] ranged between 516.4 and 517.4 eV, whereas the next oxidation state, V(IV), represented by V₂O₄, showed values in the range of 515.4-515.7 eV.¹⁰ The deconvoluted peaks for VTi30 and VTi40 indicated that these samples

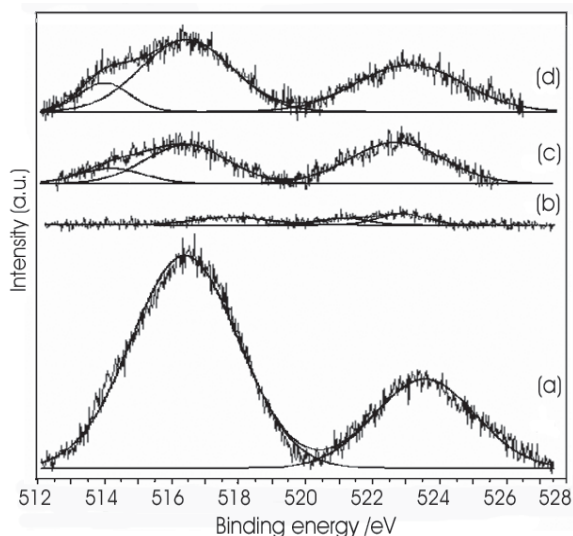


Fig 5. V 2p XPS spectra of (a) sV2O5, (b) VTi03, (c) VTi30 and (d) VTi40.

consisted of a dispersed vanadium oxide phase on the surface of the support with some V(IV) but mostly V(V) due to the higher peak area for the latter. These results suggested that the supported V(V) state is partially reduced to V(IV) state, as proposed in the literature.² The broadening of the XPS peaks can be attributed to various factors including (i) the presence of more than one type of V(V) or V(IV) species with different chemical characteristics, which cannot be discerned by XPS, and (ii) the electron transfer between the active component and the support (metal oxide-support interaction).¹

Table 3. The binding energies and the percentage area of each peak (in parentheses) of the cerium species on TiO₂ (anatase).

Cerium sample	Ce (v') (A %)	Ce (v'') (A %)	Ce (u') (A %)	Ce (u'') (A %)
CTi22	885.0 (24.1)	889.0 (15.8)	904.1 (46.9)	907.8 (9.0)
CTi30	885.2 (26.3)	889.0 (19.8)	903.6 (29.8)	907.5 (23.9)
CTi40	885.0 (20.3)	889.0 (23.1)	903.3 (22.7)	907.4 (33.8)

Table 3 shows the binding energies and the percentage area of each peak for each cerium species CTi22, CTi30 and CTi40, after deconvolution. According to Burroughs *et al.*,¹⁶ Ce(v'), Ce(v''), Ce(u') and Ce(u'') can be attributed to cerium oxides, which are the results of hybridization between the O 2p level and the Ce 4f screening level; v' are a mixture of Ce (5d 6s)⁰ 4f², O 2p⁴ and Ce (5d 6s)⁰ 4f¹, O 2p⁵ configurations,

corresponded to Ce(II) and Ce(III) respectively, while v'' is the Ce $(5d\ 6s)^0\ 4f^1\ O\ 2p^5$ final state, corresponded to Ce(III). The v structures are due to the Ce $3d_{5/2}$ levels in Ce_2O_3 , and the u structures, due to the Ce $3d_{3/2}$ levels, can be explained in the same way. The accuracy of such an analysis can be estimated to be about 5%. The mean energy level differences between the Ce $3d_{5/2}$ levels and the Ce $3d_{3/2}$ levels of both $v'-u'$ and $v''-u''$ were 18.6 eV. The equal values of the mean energy level differences between the Ce $3d_{5/2}$ levels and the Ce $3d_{3/2}$ levels of $v'-u'$ and $v''-u''$, supported the assumption that the two hybridizations are reasonable due to the same separation energy values between Ce $3d_{5/2}$ and the Ce $3d_{3/2}$ levels. Only the reference CeO_2 showed the pure Ce(IV) peak at 918.9 eV compared to the value of 917.5 eV in the literature.⁴ It has been reported that the detection of pure CeO_2 by XPS is difficult because some oxygen atoms at the surface are very labile in ultra high vacuum and under the X-ray beam, leading to about 5-8% of apparent reduction. However, the mixed oxide was easily destroyed even at 573 K under air, as confirmed by the temperature programmed reduction – temperature programmed oxidation (TPR-TPO) experiment.⁴

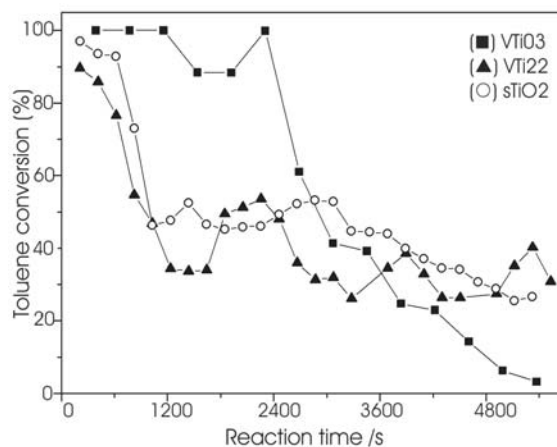
BET Surface Area

The surface areas of VTi03 VTi22 VTi40 CTi03 CTi22 CTi40 are shown in Table 4.

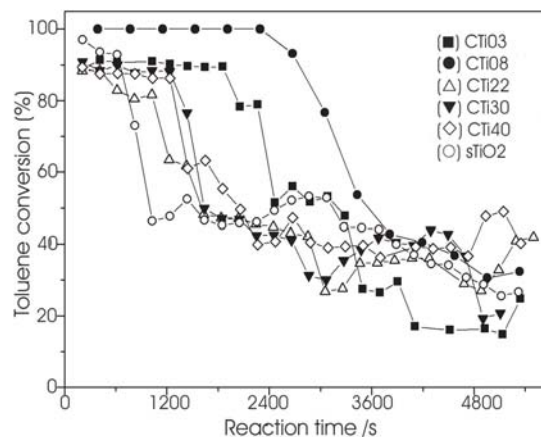
Table 4. The surface areas of VTi03 VTi22 VTi40 CTi03 CTi22 and CTi40.

Catalyst	Surface area (m^2g^{-1})
sTiO ₂	24.54
VTi03	31.82
VTi22	21.63
VTi40	23.01
CTi03	78.29
CTi08	48.06
CTi40	18.15

The surface area of CTi03 was the highest, whereas the values of the vanadium containing species were almost the same as that of sTiO₂. The assumption is that the cerium species is well dispersed in the hole between octahedral TiO₆ units of anatase, making the anatase more porous during calcination. With the higher loaded cerium samples, the surface area dropped significantly, confirming that the cerium species in the lower cerium content samples, such as CTi03, made the anatase more porous than that of the higher cerium content samples, such as CTi40.



(a)



(b)

Fig 6. Percentage conversion of toluene during the course of oxidation reaction in the presence of fresh catalysts (pretreated 1 h):

(a) VTi03, VTi22 and sTiO₂.

(b) CTi03, CTi08, CTi22, CTi30, CTi40 and sTiO₂.

Catalytic Oxidation of Toluene

Figure 6 (a) shows the percentage conversion of toluene oxidation in the presence of the fresh catalysts; VTi03, VTi22 compared to the results for the reference TiO₂ (sTiO₂). Figure 6 (b) shows the percentage conversion of toluene oxidation in the presence of fresh CTi03, CTi08, CTi22, CTi30 and CTi40, also compared to the results for the reference TiO₂ (sTiO₂). All catalysts were pretreated in flowing air ($85\ cm^3\ min^{-1}$) at 723 K for 1 h. VTi03 oxidized toluene better than VTi22. The results from VTi03 were better than those from the reference TiO₂, which oxidized toluene with more than 90% conversion in 2400 s. CTi08

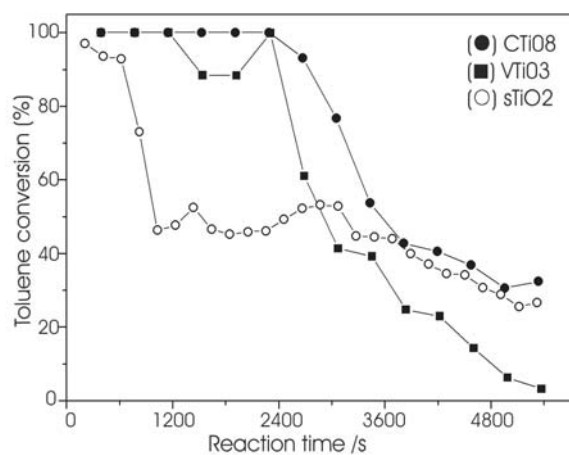
oxidized toluene closed to 100% conversion within the first 2400 s, which was better than CTi03 CTi22 CTi30 CTi40 and sTiO₂ [Figure 6(b)]. However, the higher loaded cerium species on titanium oxide showed catalytic activities of 90-60% conversion between 800-1200 s, and the reference TiO₂ (sTiO₂) showed the activities of 70-45% conversion over the same period of time.

It has been reported that the site of activity of a V/Ti-oxide catalyst is the V-O-Ti bond.¹⁷ The VTi03 catalyst oxidized toluene much better than VTi22, which confirms the V-O-Ti bond activity. Some V₂O₅ in VTi22 caused less activity. Sample CTi08, with higher cerium content than CTi03, showed better performance due to more Ce-O-Ti bonds. However, the higher cerium

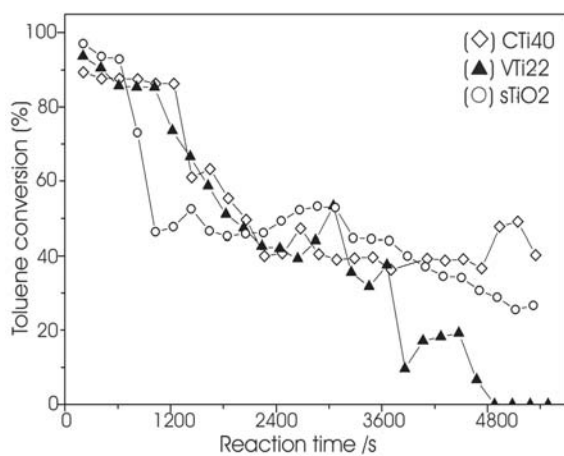
content catalysts, such as CTi22 CTi30 and CTi40, also showed lower activities. It may be assumed that the higher cerium content samples with some Ce-O-Ce as interstitial species in anatase caused less activity. The performances of the regenerated catalysts were in the same range as those of the fresh catalysts but with a little lower percentage conversion of toluene.

The activities of cerium and vanadium species were compared using CTi08-VTi03 and CTi40-VTi22, with the mole ratio of 0.03 and 0.2 of cerium (or vanadium) to titanium, respectively (Table 1, Figures 7(a) and 7(b)). Both CTi08 and VTi03 performed well within the first 1200 s. CTi08 still had good performance after that period. The catalytic activities of both CTi08 and VTi03 were higher than that of the reference sTiO₂ during the period of 3000 s. CTi40 and VTi22 were pretreated with flowing air (85 cm³ min⁻¹) at 823 K for 3 h before each reaction. They had better activities than those oxidized in air at 723 K for 1 h. The percentage conversions of toluene in the presence of VTi22 during the first 1200 s increased from 30-85% to 70-85% when the catalyst pretreatment was changed from 1 h to 3 h. CTi40 produced the same trend such that the percentage conversions of toluene during the same period increased from 85% to 85-90% when the catalyst pretreatment was changed from 1 h to 3 h. It can be assumed that upon catalyst pretreatment under flowing air at 823 K for 3 h, the activities of CTi40 and VTi22 were much better due to the production of more active Ce(IV) and V(V) by Ce(III) and V(IV) oxidation. Thus, the higher oxidation states of both cerium and vanadium play an important role in catalytic activity. Sample CTi40, with the same mole ratio of cerium to titanium as in sample VTi22, oxidized toluene with the same activities (Figure 6(b)) and was active for a period of 1200 s. After 4800 s, the cerium samples still had high activities up to 40% conversion, whereas the vanadium site was no longer active.

According to the literature,¹⁷ the oxygen species (O²⁻) in bridging oxygen of V-O-Ti bonds are responsible for hydrocarbon oxidation, and bulk V₂O₅ has low activity in selective toluene oxidation. Samples CTi08 - VTi03 and CTi40 - VTi22 had comparable performances for toluene oxidation, showing 100% conversion for 2400 s and 90% conversion for 1200 s respectively. By comparison, sTiO₂ shows 90-100% conversion in the first 10 min. It can therefore be proposed that Ce-O-Ti and V-O-Ti bonds were the active sites in the catalytic oxidations. Cerium and vanadium, with the same mole ratios to titanium, performed the same function. The results for sTiO₂ showed that Ti-O-Ti bonds were also active in this regard, but they were deactivated easily. According to the Mars-van Krevelen mechanism,¹⁸ a bridging oxygen between Ti and Ce (or V) is responsible for C-H (of the



(a)



(b)

Fig 7. Percentage conversion of toluene during the course of oxidation reaction in the presence of fresh catalysts: (a) pretreated 1 h; CTi08, VTi03 and sTiO₂. (b) pretreated 3 h; CTi40, VTi22 and sTiO₂.

methyl group of toluene) activation by abstracting hydrogen. Oxygen atom from Ti-O species attacks the forming carbocation leading to an adsorbed toluene on the metal oxide surface. It can be assumed that the product formation occurs via an electron transfer mechanism. The desorption and oxidation processes leave a vacant site and reduced species, namely, Ce(III), V(IV) and Ti(III). Cerium and vanadium, which are deposited in anatase as interstitial particles, can transfer an electron more easily than the titanium ion in the crystalline anatase. As a consequence, TiO₂ (anatase) alone (sTiO₂) was deactivated easily with less reoxidation.

Catalytic Selectivity

The selectivities for the major toluene oxidation products, namely benzaldehyde, benzene and methanol as a function of reaction time are shown in Figures 8 and 9, together with the percentage conversion of toluene. The selectivities towards methanol, benzene and benzaldehyde are close to zero when toluene was oxidized over CTi08, with almost 100% conversion for 2400 s. The selectivity towards benzaldehyde formation increased to 5% (Figure 8b) when the percentage conversion of toluene decreased. VTi03 performed with the same trend as CTi08, with

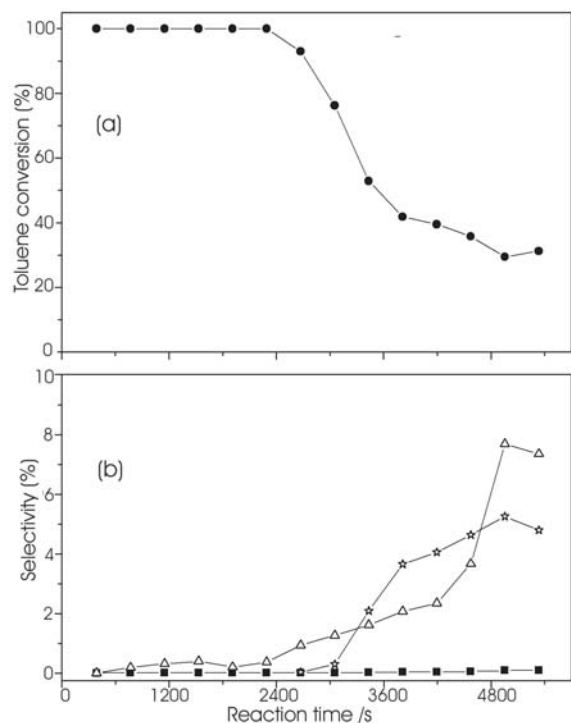


Fig 8. Percentage conversion (a) and product selectivity (b) of toluene during the course of oxidation reaction in the presence of CTi08: Toluene (●), methanol (■), benzene (Δ) and benzaldehyde (★).

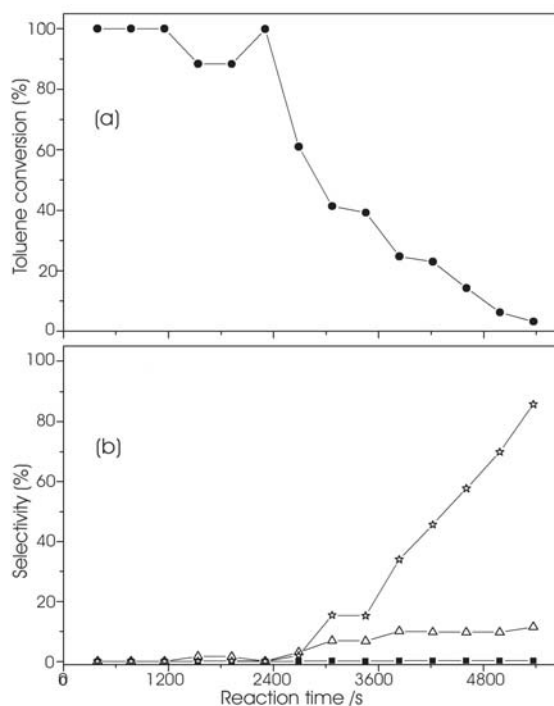


Fig 9. Percentage conversion (a) and product selectivity (b) of toluene during the course of oxidation reaction in the presence of VTi03: Toluene (●), methanol (■), benzene (Δ) and benzaldehyde (★).

the exception that the selectivities towards benzaldehyde and benzene formation were 80 and 10%, respectively.

Ce(III) was oxidized easily, as confirmed by XPS, the pretreatment results and the TPR-TPO experiment,⁴ which kept the oxide of the Ce-O-Ti bond active for the oxidative destruction of the arene ring for a long period. Partial oxidation to benzaldehyde was observed when VTi03 was deactivated after use for 1800 s. The vanadium species was assumed to be in the less active state, such as V(IV), with some adsorbed reduced species, such as coke, which made V(IV) more difficult to be oxidised.

CONCLUSIONS

The cerium/TiO₂ (anatase) and vanadium/TiO₂ (anatase) prepared via the sol-gel method mainly contained the active anatase phase of TiO₂ according to the XRD patterns. The results from Raman spectroscopy, supported the proposal that both species formed M-O-Ti bonds (M = Ce or V) on the anatase. The catalytic activities of the cerium species were comparable to those of the well known V/TiO₂ when the same mole ratios of the prepared catalysts were used. It is assumed that the oxygen of the M-O-Ti bonds (M = Ce or V) together with the high oxidation states

of Ce(IV) and V(V) played the crucial role in the oxygen transfer step. It can be concluded from the high performance catalysts that the cerium species on TiO₂ (anatase) oxidised the arene ring readily with hydrocarbon selectivity close to zero and remained active for 3600 s. The results also confirmed that Ce(III) is reoxidised more easily, forming active Ce-O-Ti bonds for aromatic destruction. In contrast, the partially deactivated vanadium/TiO₂ (anatase) produced benzaldehyde as a major product from the partial oxidation of toluene.

ACKNOWLEDGEMENTS

The authors acknowledge support from the Kasetsart University Research Institute, Thailand, and Deutscher Akademischer Austauschdienst (DAAD), Germany. We thank Dr. P. Songsiriritthigul for the technical advice of XPS measurement at the Siam Photon Laboratory, Thailand.

REFERENCES

- Reddy BM, Srekanth PM, Reddy CP, Yamada Y, Xu Qiang, Sakurai H and Kobayashi T (2002) Surface characterization of La₂O₃-TiO₂ and V₂O₅/La₂O₃-TiO₂ catalysts. *J Phys Chem B* **106**, 5695-700.
- Bulushev DA, Kiwi-Minsker L, Zaikovskii VI and Renken A (2000) Formation of active sites for selective toluene oxidation during catalyst synthesis via solid-state reaction of V₂O₅ with TiO₂. *J Catal* **193**, 145-53.
- Francisco MSP, Mastelaro VR, Nascente PAP and Florentino AO (2001) Activity and characterization by XPS, HR-TEM, Raman spectroscopy and BET surface area of CuO/CeO₂-TiO₂ catalysts. *J Phys Chem B* **106**, 10515-22.
- Rynkowski J, Farbotko J, Touroude R and Hilaire L (2000) Redox behaviour of ceria titania mixed oxide. *Appl Catal A: General* **203**, 335-48.
- Holgado JP, Alvarez R and Munuera G (2000) Study of CeO₂ XPS spectra by factor analysis: reduction of CeO₂. *Appl Surf Sci* **161**, 301-15.
- Bulushev DA, Kiwi-Minsker L and Renken A, (2000) Vanadia/titania for gas phase partial toluene oxidation spectroscopic characterization and transient kinetics study. *Catalysis Today* **57**, 231-9.
- Sax NI (1979) *Dangerous Properties of Industrial Materials*, 5th ed, pp 1035. Van Nostrand Reinhold, New York.
- Songsiriritthigul P, Pairsuwan W and Ishii T (2001) Photoemission beamline at the Siam Photon Laboratory. *Surf Rev Lett*, **8**, 497.
- Diebold U (2003) The surface science of titanium dioxide. *Surf Sci Rep* **48**, 53-229.
- Roozeboom F, Mittelmeijer-Hazeleger MC, Moulijn JA, Medema J, de Beer VH and Gellings PJ (1980) Vanadium oxide monolayer catalysts: A Raman spectroscopic and temperature programmed reduction study of monolayer and crystal type vanadia on various supports. *J Phys Chem* **84**, 2783-91.
- Francisco MSP and Mastelaro VR (2002) Inhibition of the anatase-rutile phase transformation with addition of CeO₂ to CuO-TiO₂ system: Raman spectroscopy, X-ray diffraction and textural studies. *Chem Mater* **14**(6), 2514-8.
- Reddy BM, Ganesh I, Reddy EP, Fernández A and Smirniotis PG (2001) Surface characterization of Ga₂O₃-TiO₂ and V₂O₅/Ga₂O₃-TiO₂ catalysts. *J Phys Chem B* **105**, 6227-35.
- Satsuma A, Takenaka S, Tanaka T, Nojima S, Kera Y, Miyata H and (2002) Studies on the preparation of supported metal oxide catalysts using JCR-reference catalysts; II Vanadia-titania catalyst: effect of starting solution and phase of titania. *Appl Catal A: General* **232**, 93-106.
- Besselmann S, Löffler E and Muhler M (2000) On the role of monomeric vanadyl species in toluene adsorption and oxidation on V₂O₅/TiO₂ catalysts: A Raman and in situ DRIFTS study. *J Molecular Catal A: Chemical* **162**, 401-11.
- Briggs D and Seah MP (Eds.) (1983) *Practical Surface Analysis by Auger and X-Ray Photoelectron Spectroscopy*, Wiley, New York.
- Burroughs P, Hammett A, Orchard AF and Thornton GJ (1976) *J Chem Soc Dalton Trans* **17**, 1686.
- Bulushev DA, Kiwi-Minsker L, Zaikovskii VI, Lapina OB, Ivanov AA, Reshetnikov SI and Renken A (2000) Effect of potassium doping on the structure and catalytic properties of V/Ti oxide in selective toluene oxidation. *Appl Catal A: General* **202**, 243-50.
- Chorkendorff I and Niemantsverdriet JW (2003) *Concepts of modern catalysis and kinetics*. pp 372. Wiley-VCH, Weinheim.